Supplementary Information for

A New Class of Ultrastable Dual Hydrogen-Bond-Donor COF for Improving the Reaction Activity

Hui-Chao Ma*, Ming-Zhe Li, Ling-Xu Zhang, Run-Min Wang, Jie Zou, Gong-Jun Chen*,

and Yu-Bin Dong

College of Chemistry, Chemical Engineering and Materials Science, Collaborative Innovation Center of Functionalized Probes for Chemical Imaging in Universities of Shandong, Key Laboratory of Molecular and Nano Probes, Ministry of Education, Shandong Normal University, Jinan 250014, P. R. China.

Email: huichaoma@sdnu.edu.cn; gongjchen@126.com.

Contents

1. Materials and instruments

The reagents and solvents employed were commercially available and used without further purification. 1,3,6,8-tetrakis(4-formylphenyl)pyrene (TFPPy)[1] and 1,4-phenylenediurea (BDU)[2] monomers were prepared according to the reported methods.

The powder diffractometer (XRD) patterns were collected by a D8 ADVANCEX-ray with Cu Kα radiation (λ = 1.5405 Å). The total surface areas of the catalysts were measured by the BET (Brunauer–Emmer–Teller) method using N_2 adsorption at 77 K, this was done by the Micromeritics ASAP 2000 sorption/desorption analyzer. TEM (Transmission electron microscopy) analysis was performed on a JEOL 2100 Electron Microscope at an operating voltage of 200 kV. Scanning electron microscopy (SEM) images were taken on a SUB010 scanning electron microscope with acceleration voltage of 20 kV. Elemental analyses for C, H and N were obtained on a FlashSmart. Infrared (IR) samples were prepared as KBr pellets, and spectra were obtained in the 400-4000 cm^{-1} range using a Perkin-Elmer 1600 FTIR spectrometer. ^{13}C solid-state NMR spectra were recorded on a MERCURY plus 400 spectrometer operating at resonance frequencies of 400 MHz. Thermogravimetric analyses (TGA) were carried out under flowing nitrogen at a heating rate of 10 °C·min^{-1} on a TA Instrument Q5 analyzer. High-resolution mass spectrometry (HRMS) analysis was carried out on a Bruker maXis ultrahigh-resolution-TOF mass spectrometer. X-ray photoelectron spectroscopy (XPS) spectra were obtained from PHI Versaprobe II.

2. Model Reaction

1-benzylidene-3-pheny lurea and *N*,1,5-triphenyl-4,5-dihydro-1*H*-1,2,4- triazol-3-amine were synthesized following the reported methods.[3]

A mixture of anisaldehyde (1.20 mL, 0.01 mol), *N*-phenylurea (1.36 g, 0.01 mol), HCl (100.00 μL, 6 M), and methanol (20.00 mL) was refluxed for 12 h. After cooling to room temperature, the resulting precipitate was collected by filtration and dried under vacuum. The crude product was purified by column chromatography on silica gel (1:1, methanol/chloroform, v/v) to yield 1-benzylidene-3-pheny lurea as a brick red solid (Yield, 73%). ESI-MS: calculated for $[M-H]^-$: 253.0168, found 253.0175. ^{1}H NMR (400 MHz, DMSO-d_6): δ 9.66 (s, 1H), 8.48 (s, 1H), 7.73 (d, *J* = 10.1, 5.6 Hz, 2H), 7.32 (d, *J* = 7.8 Hz, 3H), 6.84 (d, *J* = 9.0 Hz, 4H), 3.16 (s, 3H). ^{13}C NMR (400 MHz, DMSO-d_6): δ 166.0, 163.9, 156.3, 139.8, 136.2, 134.7, 129.4, 127.8, 124.1, 123.5, 122.1, 121.8, 119.0, 115.3, 54.9.

A mixture of 1-benzylidene-3-pheny lurea (2.54 g, 0.01 mol), phenylhydrazine (0.98 mL, 0.01 mol), KOH (0.50 g, 0.01 mol), and ethanol (20.00 mL) was refluxed for 4 h. After cooling to room temperature, the resulting precipitate was collected by filtration and dried under vacuum. The crude product was crystallized using methanol as solvent to yield *N*,1,5-triphenyl-4,5-dihydro-1*H*-1,2,4- triazol-3-amine as a light gray solid (Yield, 80%). ESI-MS: calculated for $[M+Na]^+$: 367.0025, found 367.0019. ^{1}H NMR (400 MHz, DMSO-d_6): δ 8.60 (s, 1H), 7.69 (d, *J* = 7.9 Hz, 1H), 7.56 (d, *J* = 20.0, 11.3, 5.7 Hz, 3H), 7.21 (d, *J* = 38.4 Hz, 4H), 6.85 (d, *J* = 24.3 Hz, 6H), 6.62 (s, 1H), 5.57 (s, 1H), 3.64 (s, 3H). ^{13}C NMR (400 MHz, DMSO-d_6): δ 155.6, 143.9, 136.3, 134.8, 132.0, 131.4, 130.1, 128.7, 127.8, 125.4, 124.2, 123.6, 122.5, 121.8, 119.0, 118.6, 117.3, 116.5, 115.8, 78.9, 53.2.

3. Synthesis of TB-COF and TBP-COF

A mixture of 1,3,6,8-tetrakis(4-formylphenyl)pyrene (TFPPy) (15.00 mg, 0.05 mmol), 1,4-phenylenediurea (BDU) (10.00 mg, 0.10 mmol) in a solution of *o*-dichlorobenzene/*n*-butanol/6 M acetic acid (9/1/0.1 by volume; 35.00 mL) was heated at 150°C for 5 days in a sealed Schlenk (50 mL) in N_2 to afford

corresponding TB-COF as the yellowish-green crystalline solids. After stayed in the vacuum chamber (100 °C) for 12 h, the activated samples were obtained (Yield, 66%). Elemental Analysis (%) calcd for $C_{30}H_{19}N_4O_2$: C, 77.09; H, 4.07; N, 12.00; found (%): C, 68.81; H, 3.69; N, 10.72.

A mixture of TB-COF (18.00 mg, 31.80 mmol), phenylhydrazine (PHZ) (4.80 uL, 0.45 mmol), KOH (17.80 mg, 0.32 mmol) in a solution of DMSO (0.50 mL) was heated at 150°C for 3 days in a sealed Schlenk (20 mL) in N_2 to afford corresponding TBP-COF as the yellowish-green crystalline solids. After stayed in the vacuum chamber (100 °C) for 12 h, the activated samples were obtained (Yield, 85%). Elemental Analysis (%) calcd for $C_{42}H_{31}N_8$: C, 77.90; H, 4.79; N, 17.31; found (%): C, 70.82; H, 4.49; N, 15.82.

4. Simulated structure of TB-COF and TBP-COF

Structural modeling of TB-COF and TBP-COF were generated using the Materials Studio (ver. 2018) suite of programs. The initial structure was geometry optimized using the MS $DMol_3$ module. The initial lattice was created by starting with the space group *C2*. The a and b lattice parameters (initially 46.012 Å and 33.86 Å) were estimated according to the center to center distance between the vertices of the COF (pyrene unit center to another pyrene unit center). The constructed model was geometry optimized using the Forcite module (Universal force fields, Ewald summations). Then the calculated PXRD pattern was generated with the Reflex Plus module. Finally, Pawley refinement was applied for profile fitting, producing the refined PXRD profile with the lattice parameters. TB-COF: a = 46.68 Å, b = 33.92 Å, c = 5.9 Å, $\alpha = \gamma = 90°$, $\beta = 47°$; TBP-COF: a = 44.60 Å, b = 33.84 Å, c = 5.9 Å, $\alpha = \gamma = 90°$, $\beta = 47°$.

Further the simulation on the stacking order of TB-COF was carried out:

- AB stacking in *C2* symmetry, this structure results in ≈ 2.4 nm pores.

- AA stacking (*Cmm2* symmetry) with ≈ 2.8 nm pores.

The MS Reflex Plus module was then used to calculate the PXRD pattern, AB stacking matched the experimentally observed PXRD pattern of TB-COF closely in both the positions and intensity of the reflections (*J. Am. Chem. Soc.* **2015**, *137*, 7079-7082; *Chem. Mater.* **2015**, *27*, 23, 7874-7881).

Similarly, the simulation on the stacking order of TBP-COF was carried out:

- AB stacking in *C2* symmetry, this structure results in ≈ 2.3 nm pores.

- AA stacking (*Cmm2* symmetry) with ≈ 2.7 nm pores.

The MS Reflex Plus module was then used to calculate the PXRD pattern, the PXRD analysis of TBP-COF displays characteristic peaks that are consistent with the simulated PXRD results of the staggered (AB) stacking.

5. Experimental procedure of TBP-COF-catalyzed Friedel-Crafts reaction

A mixture of *β*-nitroalkene (0.57 mmol), indole (0.84 mmol) and TBP-COF (3 mol%, 11.0 mg) in CH_2Cl_2 (1.50 mL) was stirred at room temperature for 18 h in air to afford the corresponding products. Yield was determined by ^1H NMR spectroscopy.

6. Supplementary Figures and Tables

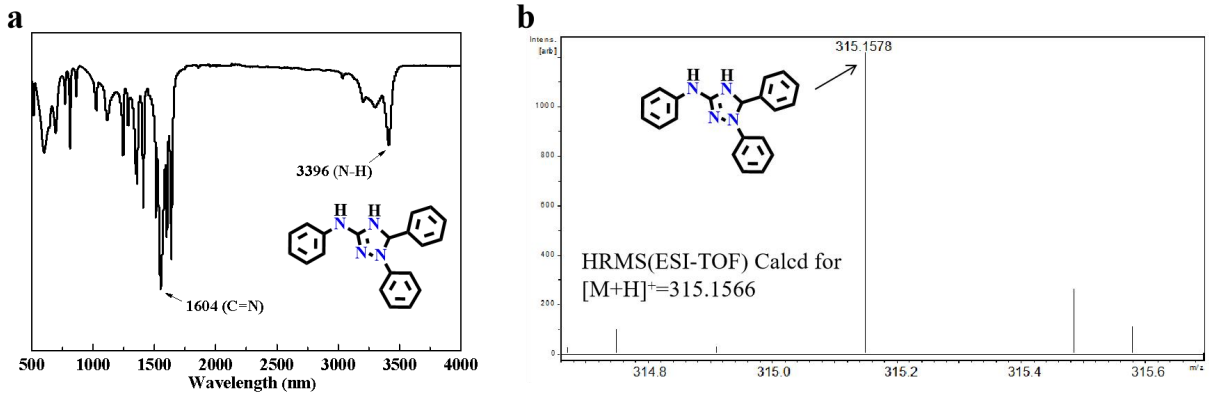

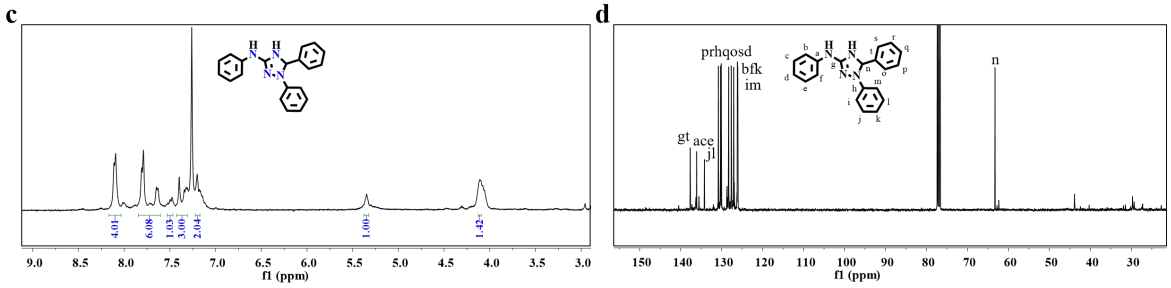

Fig. S1. Characterization of model products. **a)** FT-IR spectra, **b)** HRMS image, **c)** ^{1}H NMR, and **d)** ^{13}C NMR of *N*,1,5-triphenyl-4,5-dihydro-1*H*-1,2,4-triazol-3-amine.

Table S1. The structure model of TB-COF with *C2* mode.

TB-COF Space group: *C2* *a* = 46.68 Å, *b* = 33.92 Å, *c* = 5.9 Å *α* = 90.0°, *β* = 47°, *γ* = 90.0°			
Atom	x	y	z
C1	0.8205	0.21414	-1.94322
C2	0.82875	0.25474	-1.95516
C3	0.80611	0.28088	-1.96572
H4	0.83738	0.19248	-1.94162
H5	0.81155	0.31223	-1.98811
C6	0.68947	0.14255	-1.86616
N7	0.70071	0.17907	-1.97145
C8	0.72729	0.17603	-1.91597
N9	0.73968	0.21506	-2.00285
O10	0.73135	0.15158	-1.78824
H11	0.69029	0.12237	-1.72825
H12	0.73303	0.23559	-2.09315
C13	0.77549	0.26614	-1.96549
C14	0.76703	0.22555	-1.95116
C15	0.78956	0.19942	-1.93932

H16	0.7599	0.28772	-1.98194
H17	0.78621	0.16794	-1.94097
C18	0.87815	0.35179	-0.92659
N19	0.89048	0.3148	-0.99416
C20	0.85586	0.30552	-0.95044
N21	0.86429	0.26528	-0.99813
O22	0.8271	0.3242	-0.85409
H23	0.88853	0.25058	-1.06161
C24	0.49013	-0.03652	-0.02144
C25	0.52147	-0.03678	-0.02282
C26	0.47509	-0.0714	-0.0386
H27	0.48774	-0.09958	-0.0628
C28	0.42618	0.0362	-0.02278
C29	0.39483	0.03647	-0.02128
C30	0.44465	0.07105	-0.04564
H31	0.43637	0.09917	-0.07221
C32	0.56577	0.05903	0.03841
C33	0.53595	0.0678	0.0372
C34	0.53085	0.10831	0.01733
C35	0.49015	0.03676	-0.02579
C36	0.5215	0.03759	-0.02723
C37	0.5548	0.13792	-0.0115
C38	0.58493	0.12934	-0.01551
C39	0.58975	0.08893	0.0115
C40	0.47515	0.07132	-0.04708
H41	0.57074	0.02862	0.05922
H42	0.54929	0.1683	-0.02828

H43	0.61221	0.08025	0.00977
H44	0.50757	0.11753	0.03035
H45	0.48782	0.09963	-0.07463
C46	0.42616	-0.03708	-0.01843
C47	0.3948	-0.0379	-0.01687
C48	0.44459	-0.07167	-0.03717
H49	0.43629	-0.10004	-0.06039
C50	0.47437	-0.00001	-0.01836
C51	0.53577	0.00053	-0.02741
C52	0.44116	-0.0003	-0.0168
C53	0.38083	-0.00085	-0.02013
C54	0.93931	0.44488	-0.12849
C55	0.95118	0.43601	0.03382
C56	0.93628	0.4003	0.20242
C57	0.91246	0.37447	0.1998
C58	0.90106	0.38282	0.03477
C59	0.91504	0.41895	-0.12939
H60	0.94901	0.47217	-0.25762
H61	0.90247	0.34747	0.33279
H62	0.90752	0.42717	-0.26059
H63	0.94236	0.39241	0.34382
C64	0.84796	0.54982	-2.05715
C65	0.87557	0.56535	-2.04784
C66	0.87764	0.60694	-2.05101
C67	0.85489	0.63134	-2.07405
C68	0.82783	0.61606	-2.08843
C69	0.8248	0.57445	-2.07821

H70	0.84357	0.5166	-2.04781
H71	0.85917	0.66455	-2.08084
H72	0.8036	0.55971	-2.0867
H73	0.89801	0.62201	-2.03481

Table S2. The structure model of TBP-COF with *C2* mode.

TBP-COF Space group: *C2* *a* = 46.60 Å, *b* = 33.84 Å, *c* = 5.9 Å *α* = 90.0°, *β* = 47°, *γ* = 90.0°			
Atom	x	y	z
C1	1.38211	1.07186	-5.4865
C2	1.41383	1.0759	-5.48017
C3	1.42696	1.11641	-5.47491
C4	1.40836	1.15286	-5.47598
C5	1.37665	1.14882	-5.48231
C6	1.36352	1.10831	-5.48757
H7	1.37219	1.04128	-5.49048
H8	1.41827	1.18345	-5.47201
C9	1.22345	1.27988	-5.47909
C10	1.27738	1.26276	-5.46996
C11	1.25381	1.29308	-5.47239
C12	1.31762	1.12701	-5.4864
C13	1.33746	1.09394	-5.49461
C14	1.32695	1.05459	-5.50321
C15	1.29661	1.04832	-5.5036
C16	1.27677	1.0814	-5.49539
C17	1.28727	1.12074	-5.48679
C18	1.35775	1.18441	-5.48874
N19	1.35715	1.22991	-5.487

C20	1.32624	1.24338	-5.49456
N21	1.30774	1.2062	-5.50097
H22	1.4509	1.11947	-5.47013
H23	1.20565	1.30276	-5.48093
H24	1.25895	1.32593	-5.46918
H25	1.28824	1.01699	-5.51045
H26	1.2526	1.0764	-5.49569
H27	1.27147	1.14709	-5.48025
H28	1.37709	1.24669	-5.48106
N29	1.32722	1.16975	-5.49737
H30	1.34275	1.02825	-5.50975
N31	1.19157	1.21798	-5.52028
H32	1.1821	1.18936	-5.54321
C33	1.11658	1.42636	-5.51309
C34	1.08486	1.42232	-5.51942
C35	1.07173	1.38181	-5.52468
C36	1.09033	1.34536	-5.52361
C37	1.12204	1.3494	-5.51728
C38	1.13517	1.38991	-5.51202
H39	1.1265	1.45694	-5.50912
H40	1.08042	1.31477	-5.52758
C41	1.27148	1.21897	-5.47406
C42	1.21755	1.23609	-5.48319
C43	1.24112	1.20577	-5.48075
C44	1.18101	1.3718	-5.49626
C45	1.16286	1.40489	-5.50722
C46	1.17404	1.44425	-5.50633

C47	1.20338	1.4505	-5.49447
C48	1.22153	1.41741	-5.48351
C49	1.21035	1.37805	-5.4844
C50	1.14229	1.31419	-5.52104
N51	1.14367	1.26871	-5.52511
C52	1.17518	1.256	-5.52253
N53	1.19327	1.29363	-5.51687
H54	1.04779	1.37875	-5.52946
H55	1.28927	1.19608	-5.47222
H56	1.23598	1.17292	-5.48397
H57	1.21228	1.48185	-5.49376
H58	1.24489	1.42239	-5.47406
H59	1.22481	1.35169	-5.47567
H60	1.12377	1.25143	-5.52909
N61	1.17294	1.3296	-5.51595
N62	1.30881	1.28068	-5.49399
H63	1.32102	1.30979	-5.50932
H64	1.15959	1.47061	-5.51506
H65	0.65912	0.89297	0.49276
H66	0.6395	0.89991	0.48333
H67	0.83958	0.60525	0.50765
H68	0.86162	0.59893	0.50569
C69	0.53473	2.03854	-3.52083
C70	0.51849	2.07716	-3.52074
C71	0.51693	2.00024	-3.50821
C72	1.46844	1.96118	0.49533
C73	1.48624	1.92289	0.48271

C74	1.43284	2.03777	0.52056
C75	1.4182	1.99871	0.50767
C76	1.436	1.96042	0.49506
H77	1.47773	0.89372	0.44537
H78	1.53314	1.10623	0.44917
H79	1.38124	1.18448	-5.75283
H80	1.16526	1.31469	-5.7852
H81	1.39376	1.99814	0.50747

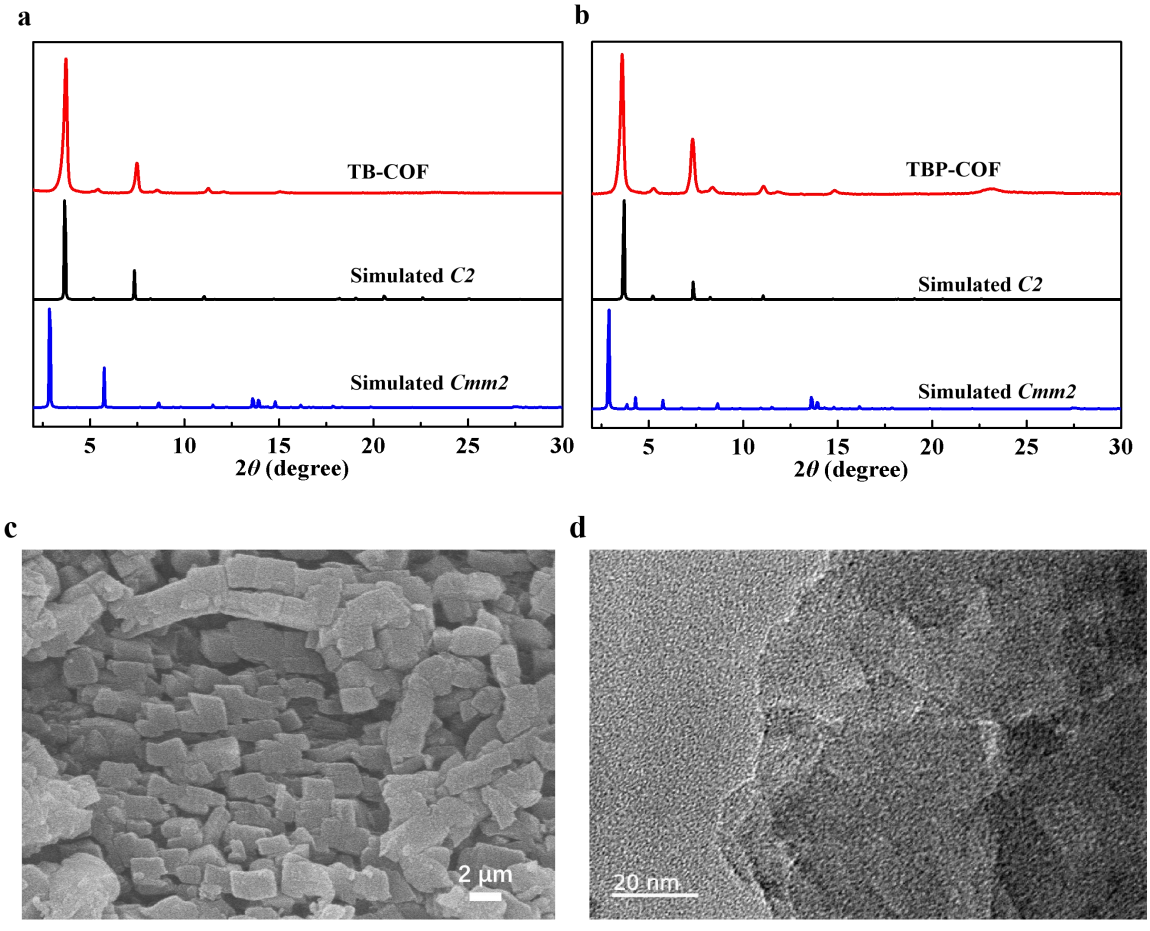

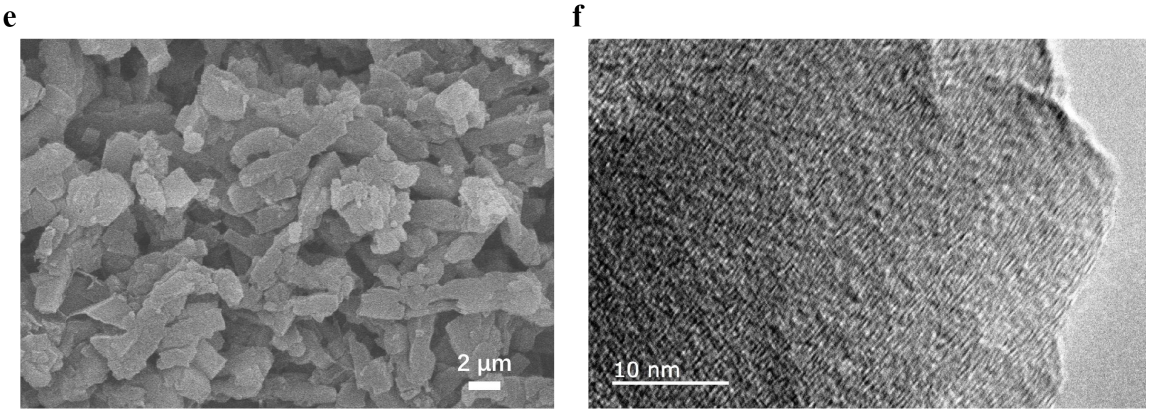

Fig. S2. The characterization of TB-COF and TBP-COF. PXRD patterns of **a)** TB-COF and **b)** TBP-COF: comparison between the experimental (red line) and the simulated patterns (black and blue lines). Compared to the pattern generated from the *Cmm2* space group (blue line), TB-COF and TBP-COF unequivocally crystallizes in the *C2* space group (black line). **c)** SEM image of TB-COF. **d)** HRTEM image of TB-COF. **e)** SEM image of TBP-COF. **f)** HRTEM image of TBP-COF.

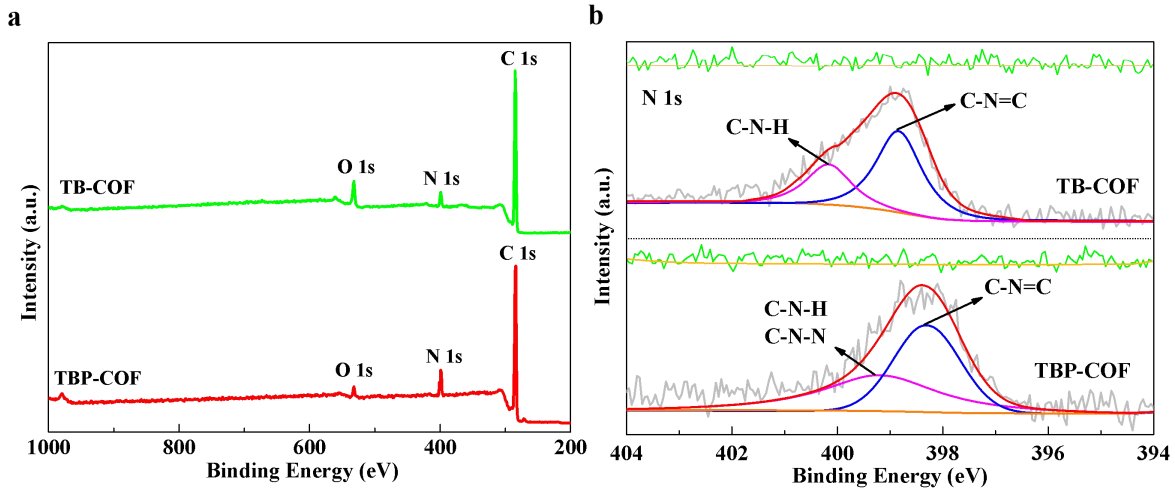

Fig. S3. a) XPS survey spectra of TB-COF and TBP-COF. **b)** XPS spectra of N 1s profile for TB-COF and TBP-COF.

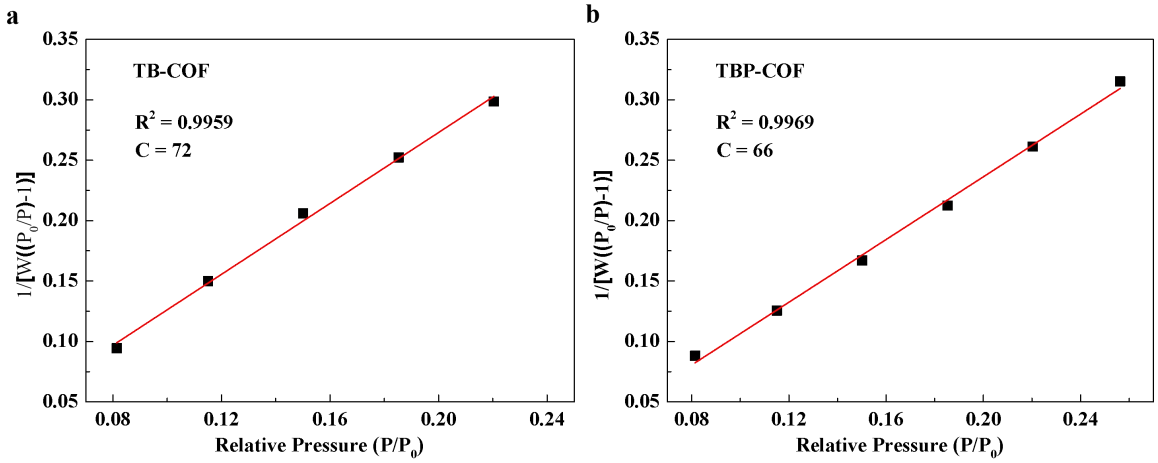

Fig. S4. BET surface area plot for **a)** TB-COF and **b)** TBP-COF.

Table S3. Optimization of TBP-COF- and TB-COF-catalysed Friedel-Crafts reaction.[a]

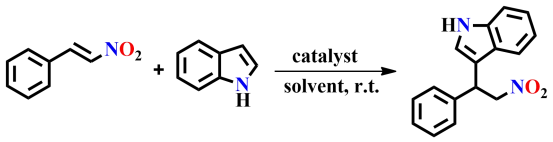

Entry	Catalyst	Solvent	Time (h)	Yield (%)[b]
1	TBP-COF (3 mol%)	CH_2Cl_2	18	99
2	TBP-COF (3 mol%)	$CHCl_3$	18	97
3	TBP-COF (3 mol%)	EtOH	18	67
4	TBP-COF (3 mol%)	PhMe	18	84
5	TBP-COF (3 mol%)	THF	18	67
6	TBP-COF (3 mol%)	Acetone	18	62
7	TBP-COF (1 mol%)	CH_2Cl_2	18	60
8	TBP-COF (1 mol%)	$CHCl_3$	18	58
9	TBP-COF (1 mol%)	EtOH	18	40
10	TBP-COF (1 mol%)	PhMe	18	50
11	TB-COF (3 mol%)	CH_2Cl_2	18	82
12	TB-COF (3 mol%)	$CHCl_3$	18	77
13	TB-COF (3 mol%)	EtOH	18	46

14	TB-COF (3 mol%)	PhMe	18	65
15	TB-COF (3 mol%)	CH_2Cl_2	24	99

[a] Reaction conditions: catalyst, *β*-nitroalkenes (0.57 mmol), indole (0.84 mmol), solvent (1.5 mL), RT, in air.

[b] Isolated yield.

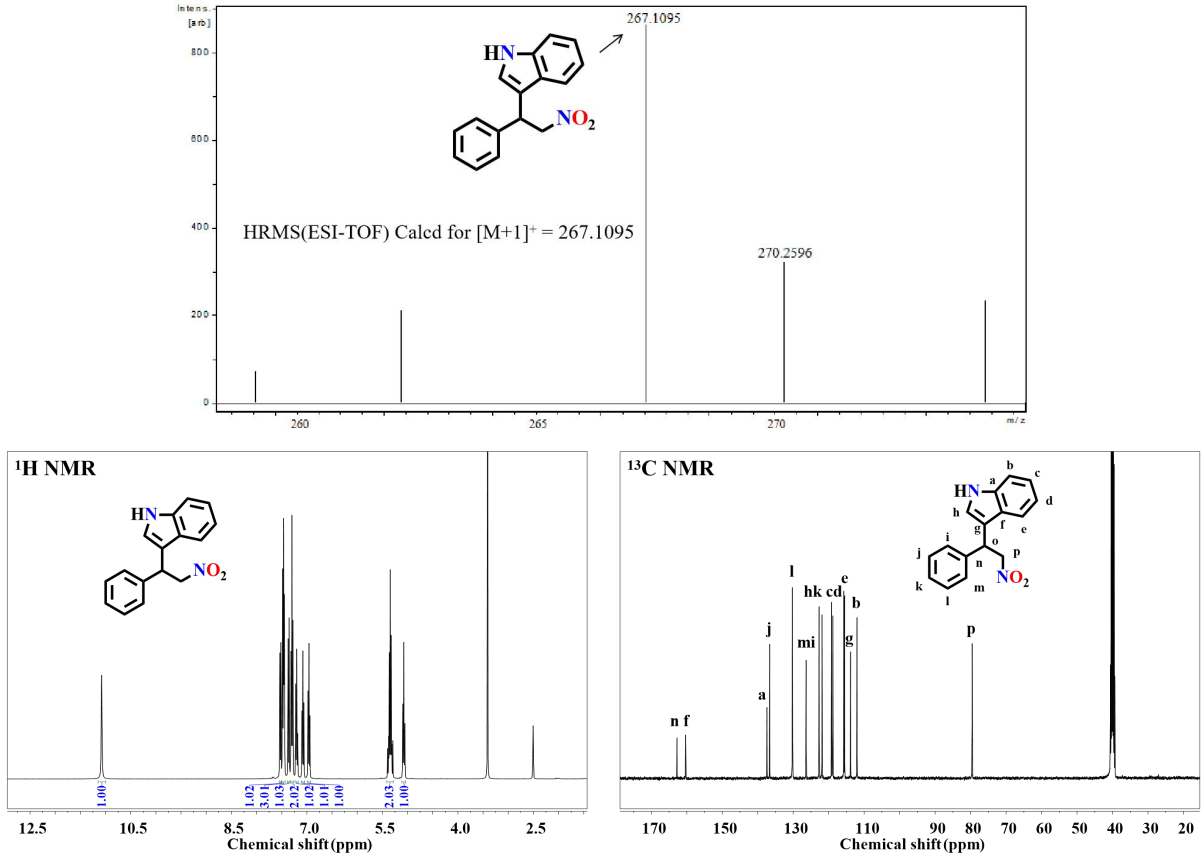

Fig. S5. The characterization of the model product catalyzed by TBP-COF. HRMS, ^{1}H NMR and ^{13}C NMR spectra for 3-(2-nitro-1-phenylethyl)-1*H*-indole obtained from Friedel-Crafts reaction based on production of *β*-nitroalkene with indole (for Table 1). HRMS (ESI): *m/z* $[M+H]^+$, Calcd for $C_{16}H_{14}N_2O_2^+$, 267.1086, found, 267.1095. ^{1}H NMR (400 MHz, DMSO-d_6): δ 11.08 (s, 1H), 7.53 (d, J = 7.9 Hz, 1H), 7.46 (dd, J = 9.2, 4.9 Hz, 3H), 7.36 (d, J = 8.1 Hz, 1H), 7.30 (t, J = 7.5 Hz, 2H), 7.20 (t, J = 7.3 Hz, 1H), 7.08 (t, J = 7.2 Hz, 1H), 6.96 (t, J = 7.3 Hz, 1H), 5.41-5.28 (m, 2H), 5.07 (t, J = 8.2 Hz, 1H). ^{13}C NMR (101 MHz, DMSO-d_6): δ 140.66, 139.03, 136.21, 128.34, 127.09, 124.11, 125.08, 121.26, 115.78, 111.47, 85.48, 46.76.

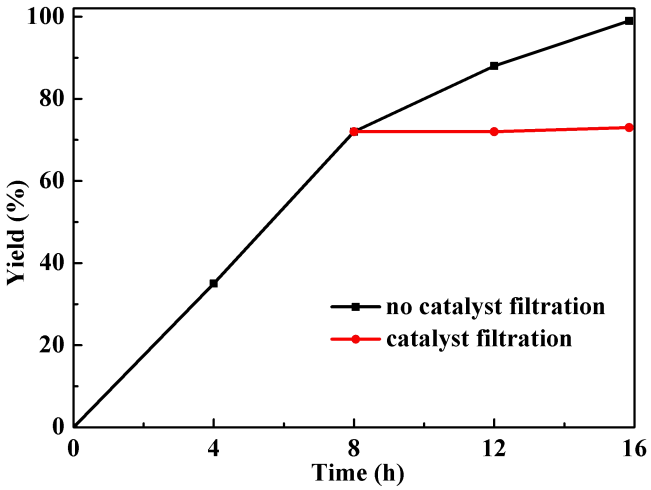

Fig. S6. The hot leaching experiment. Reaction time examination (black line) and leaching test (red line). The solid catalyst was filtrated from the reaction solution after 10 h, whereas the filtrate was transferred to a new vial and the reaction was carried out under the same conditions for an additional 8 h.

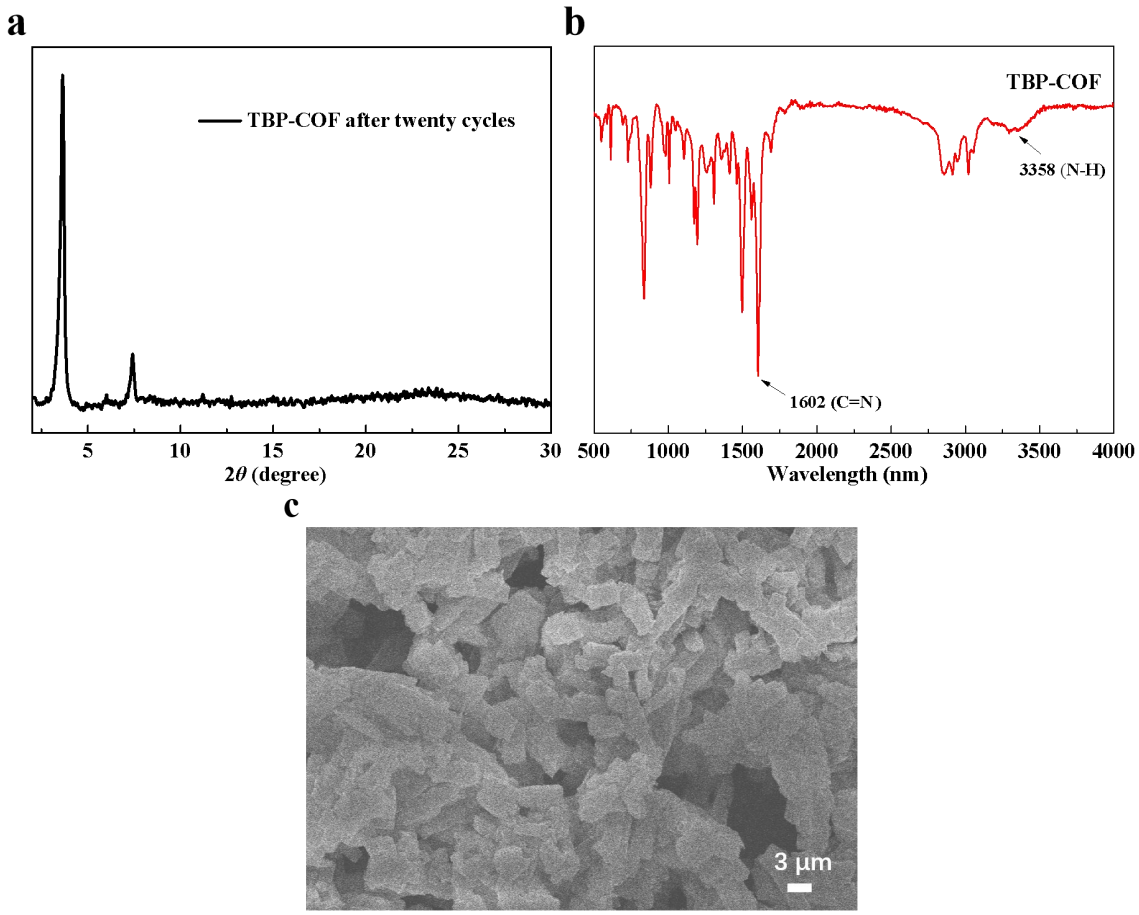

Fig. S7. The catalytic cycle stability of TBP-COF. **a)** PXRD pattern, **b)** FT-IR spectra and **c)** SEM image of

TBP-COF after twenty catalytic cycles. After each catalytic run, the solid catalyst was readily recovered by centrifugation, washed with ethanol and dichloromethane, then dried at 90°C in vacuum and reused for the next run under the same reaction conditions.

Table S4. Comparison of TBP-COF with the reported catalysts for the Friedel-Crafts reaction of *β*-nitroalkene with indole.

Catalyst	Conditions	Yield (%)	Ref
Zr(IV)-UiO-67	C_7H_8/70°C/24h	97	4
$CoCl_2·6H_2O$	Solventless/100°C/25h	97	5
MIL-101(Cr)@thiourea	C_7H_8/80°C/18h	84	6
2,6-Bis(amido)benzoic Acid	$CHCl_3$/40°C/24h	92	7
Trisulfonamide Calix[6]arene	H_2O/50°C/24h	84	8
$B(C_6F5)_3$	$CHCl_3$/80°C/24h	94	9
Zn(II)-thiourea complex	CH_3CH_2OH/r.t./48h	89	10
UiO-66(Ce)	$C_2H_4Cl_2$/80°C/24h	98	11
$Cu_2(dbda)(CH_3OH)_2$	$CHCl_3$/50°C/8h	95	12
sulfonated carbon-based solid acid	H_2O/r.t./48h	76	13
$Zn(OAc)_2·2H_2O$	C_6H_{12}/80°C/14h	97	14
N-Bromosuccinimide	CH_2Cl_2/40°C/5h	94	15
NPS-γ-Fe_2O_3	Solventless/100-101°C/1h	85	16
$FeCl_3·6H_2O$	Solventless/80°C/12h	97	17
$CeCl_3·7H_2O$-NaI-SiO_2	Solventless/r.t./8h	96	18
MOF$\{[Zn_2(2BQBG)(BDC)_2]·10H_2O\}_n$	CH_2Cl_2/35°C/12h	100	19
3-$Cu(OTf)_2$	$CHCl_3$/0°C/24h	79	20
$Cu_3(BTC)_2$	CH_4/55°C/24h	98	21
POP	EtOH/50°C/12h	87	22
CSMCRI-12	CH_4/60°C/24h	100	23

HY zeolite	Solventless/50°C/1h	95	24
CSMCRI-17	CH_3CN/60°C/12h	97	25

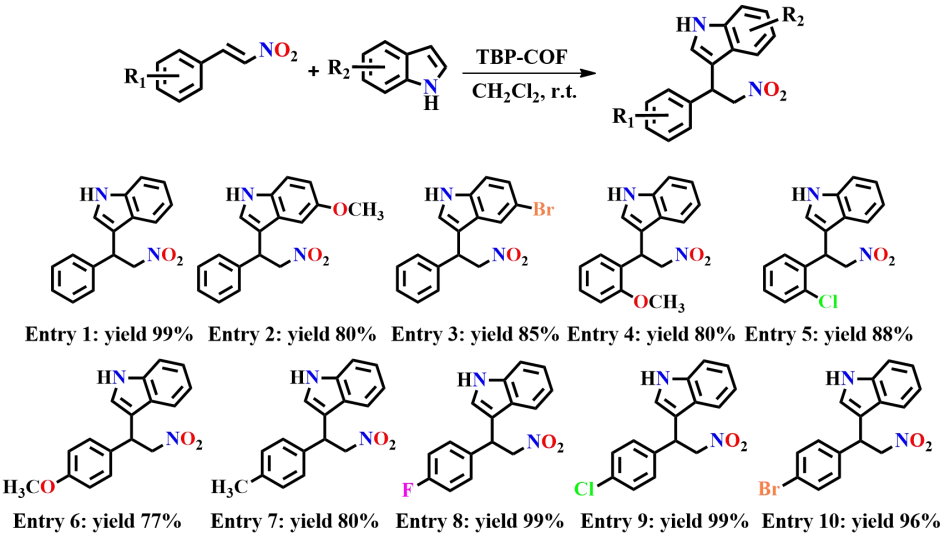

Fig. S8. Scope of TBP-COF-catalysed Friedel-Crafts reaction.[a]

[a]Reaction conditions: catalyst, *β*-nitroalkenes (0.57 mmol), indole (0.84 mmol), CH_2Cl_2 (1.5 mL), RT, 18 h, in air. [b]Isolated yield. Products were determined by ^1H NMR, ^{13}C NMR and HRMS spectra (Figures S7-15).

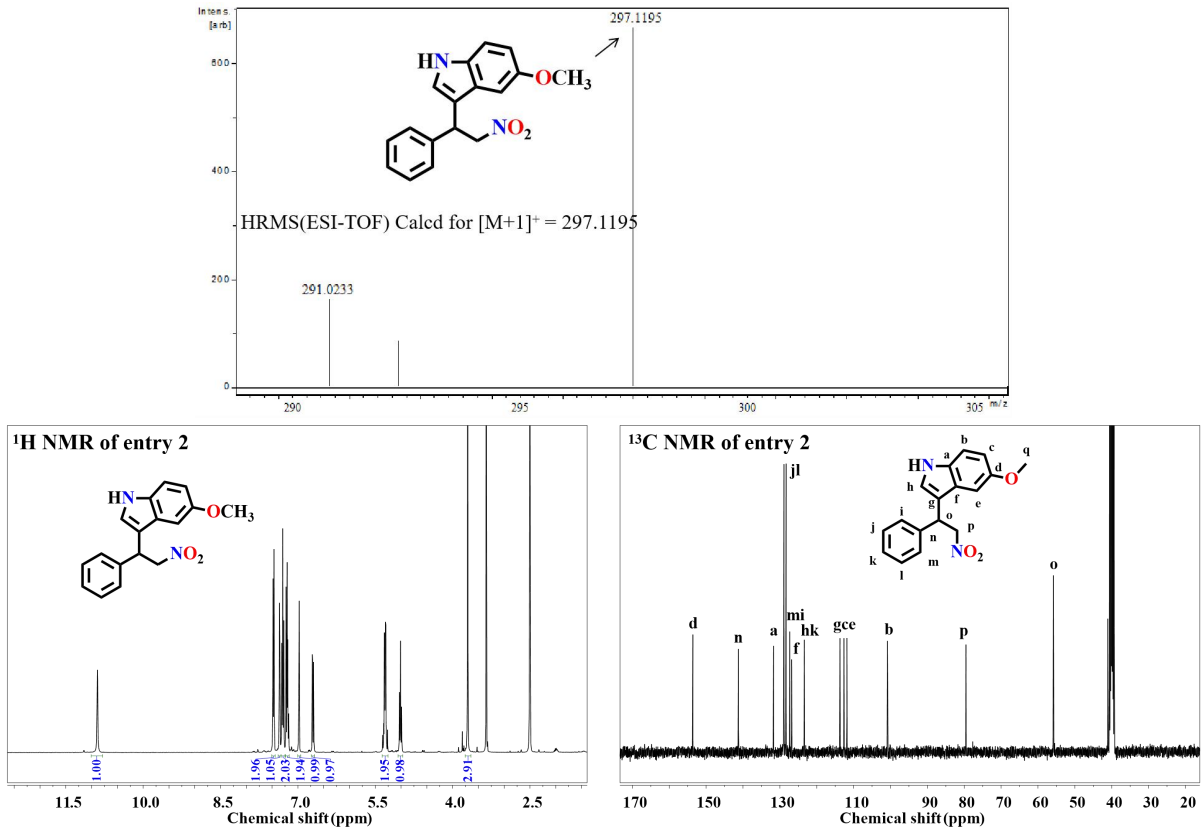

Fig. S9. HRMS, ^{1}H NMR and ^{13}C NMR spectra for 5-methoxy-3-(2-nitro-1-phenylethyl)-1*H*-indole (Table 2, entry 2). HRMS (ESI): *m/z* $[M+H]^+$, Calcd for $C_{17}H_{16}N_2O_3^+$, 297.1176, found, 297.1195. ^{1}H NMR (400 MHz, DMSO-d_6): δ 10.89 (s, 1H), 7.47 (d, J = 7.2 Hz, 2H), 7.36 (d, J = 2.5 Hz, 1H), 7.29 (t, J = 7.5 Hz, 2H), 7.24-7.17 (m, 2H), 6.98 (d, J = 2.3 Hz, 1H), 6.71 (dd, J = 8.8, 2.4 Hz, 1H), 5.37-5.25 (m, 2H), 5.01 (t, J = 8.2 Hz, 1H), 3.71 (d, J = 6.3 Hz, 3H). ^{13}C NMR (101 MHz, DMSO-d6) δ = 153.59, 141.24, 131.71, 128.89, 128.30, 127.31, 126.80, 123.36, 113.68, 112.62, 111.80, 100.84, 79.52, 55.83.

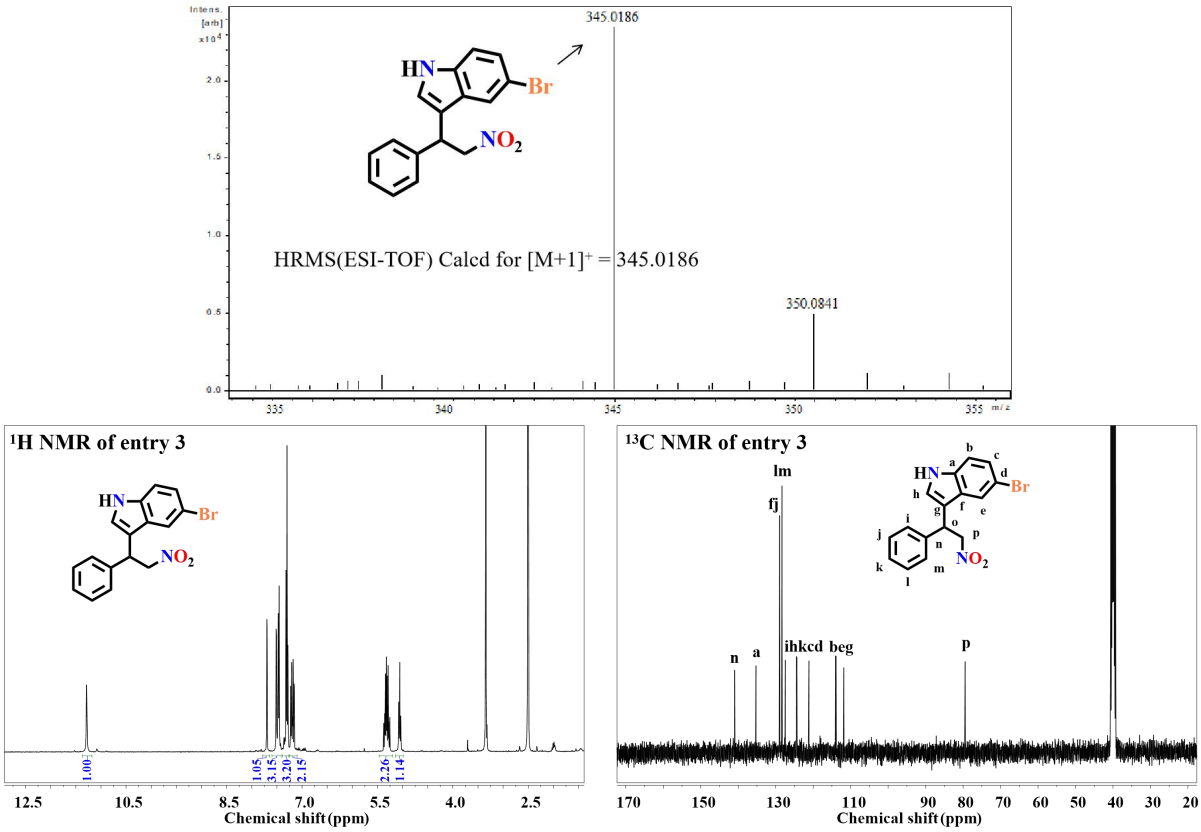

Fig. S10. HRMS, ^{1}H NMR and ^{13}C NMR spectra for 5-bromo-3-(2-nitro-1-phenylethyl)-1*H*-indole (Table 2, entry 3). HRMS (ESI): *m/z* $[M+H]^+$, Calcd for $C_{16}H_{13}BrN_2O_2^+$, 345.0185, found, 345.0186. ^{1}H NMR (400 MHz, DMSO-d_6): δ 11.29 (s, 1H), 7.70 (d, J = 1.6 Hz, 1H), 7.49 (dd, J = 18.4, 4.8 Hz, 3H), 7.30 (t, J = 7.8 Hz, 3H), 7.26-7.10 (m, 2H), 5.47-5.19 (m, 2H), 5.06 (t, J = 8.2 Hz, 1H). ^{13}C NMR (101 MHz, DMSO-d6) δ = 140.97, 135.26, 128.97, 128.32, 127.45, 124.41, 121.15, 113.96, 111.85, 79.46.

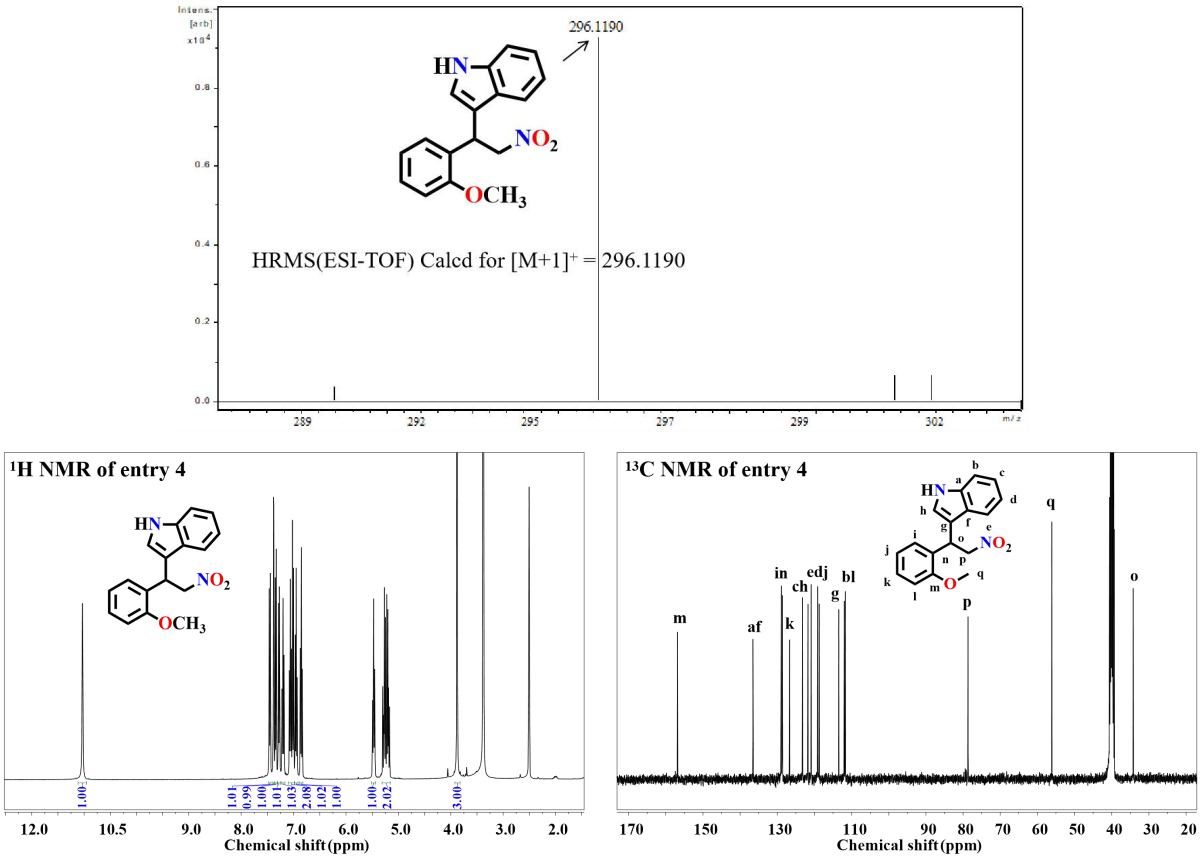

Fig. S11. HRMS, ^{1}H NMR and ^{13}C NMR spectra for 3-(1-(2-methoxyphenyl)-2-nitroethyl)-1*H*-indole (Table 2, entry 4). HRMS (ESI): *m/z* $[M+H]^+$, Calcd for $C_{17}H_{16}N_2O_2^+$, 296.1167, found, 296.1190. ^{1}H NMR (400 MHz, DMSO-d_6): δ 11.03 (s, 1H), 7.46 (d, J = 7.9 Hz, 1H), 7.38 (d, J = 2.1 Hz, 1H), 7.34 (d, J = 8.1 Hz, 1H), 7.28 (dd, J = 7.6, 1.3 Hz, 1H), 7.24-7.17 (m, 1H), 7.10-6.98 (m, 2H), 6.95 (t, J = 7.5 Hz, 1H), 6.85 (t, J = 7.4 Hz, 1H), 5.47 (t, J = 8.1 Hz, 1H), 5.23 (ddd, J = 20.6, 12.9, 8.2 Hz, 2H), 3.88 (s, 3H). ^{13}C NMR (101 MHz, DMSO-d6) δ = 156.89, 136.56, 128.90, 128.62, 126.70, 123.22, 121.74, 120.89, 119.13, 118.73, 113.45, 111.98, 111.68, 78.67, 56.12, 34.58.

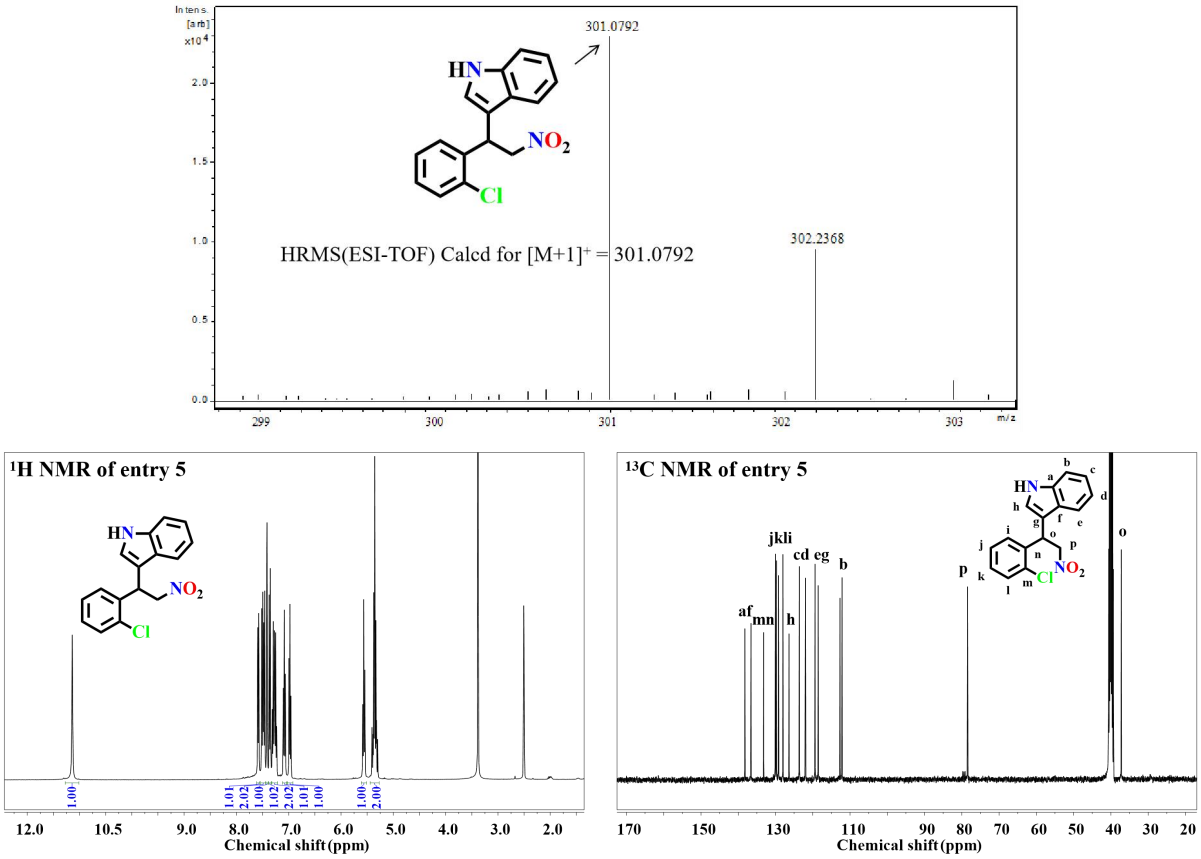

Fig. S12. HRMS, ^{1}H NMR and ^{13}C NMR spectra for 3-(1-(2-chlorophenyl)-2-nitroethyl)-1*H*-indole (Table 2, entry 5). HRMS (ESI): *m/z* $[M+H]^+$, Calcd for $C_{16}H_{13}ClN_2O_2^+$, 301.0786, found, 301.0792. ^{1}H NMR (400 MHz, DMSO-d_6): δ 11.14 (s, 1H), 7.58 (dd, J = 7.6, 1.7 Hz, 1H), 7.54-7.44 (m, 2H), 7.42 (d, J = 2.4 Hz, 1H), 7.36 (d, J = 8.1 Hz, 1H), 7.32-7.21 (m, 2H), 7.08 (t, J = 7.5 Hz, 1H), 6.98 (t, J = 7.5 Hz, 1H), 5.57 (t, J = 8.1 Hz, 1H), 5.44-5.27 (m, 2H). ^{13}C NMR (101 MHz, DMSO-d_6) δ = 138.24, 136.58, 133.19, 130.05, 129.74 , 129.18, 128.00, 126.36, 123.62, 121.96, 119.39, 118.55, 112.68, 112.15, 78.45, 37.93.

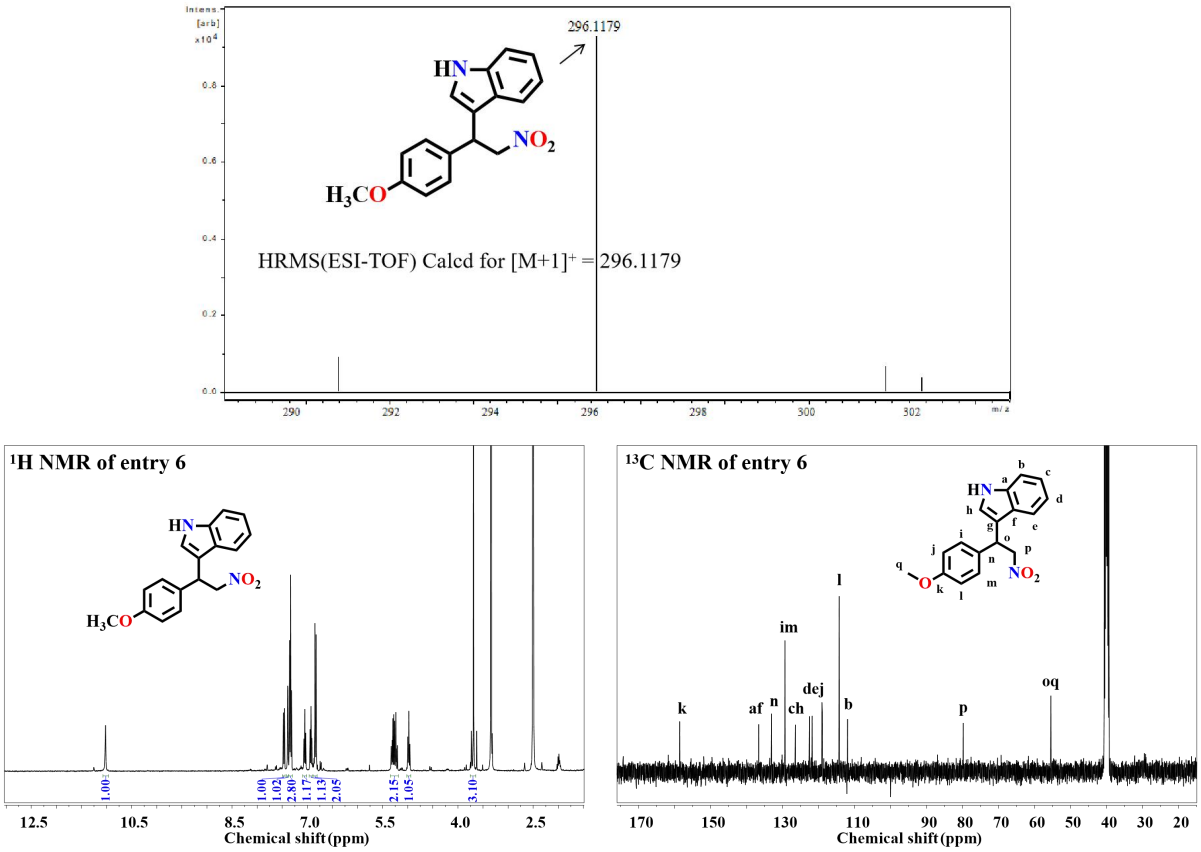

Fig. S13. HRMS, ^{1}H NMR and ^{13}C NMR spectra for 3-(1-(4-methoxyphenyl)-2-nitroethyl)-1*H*-indole (Table 2, entry 6). HRMS (ESI): *m/z* $[M+H]^+$, Calcd for $C_{17}H_{16}N_2O_2^+$, 296.1167, found, 296.1179. ^{1}H NMR (400 MHz, DMSO-d_6): δ 11.02 (s, 1H), 7.47 (d, J = 8.0 Hz, 1H), 7.39 (d, J = 2.3 Hz, 1H), 7.33 (t, J = 8.0 Hz, 3H), 7.05 (s, 1H), 6.93 (s, 1H), 6.84 (d, J = 8.7 Hz, 2H), 5.34-5.19 (m, 2H), 4.98 (s, 1H), 3.69 (s, 3H). ^{13}C NMR (101 MHz, DMSO-d_6) δ = 158.56, 136.63, 133.05, 129.34, 126.43, 122.53, 121.77, 118.99, 114.26, 111.94, 79.83, 55.45.

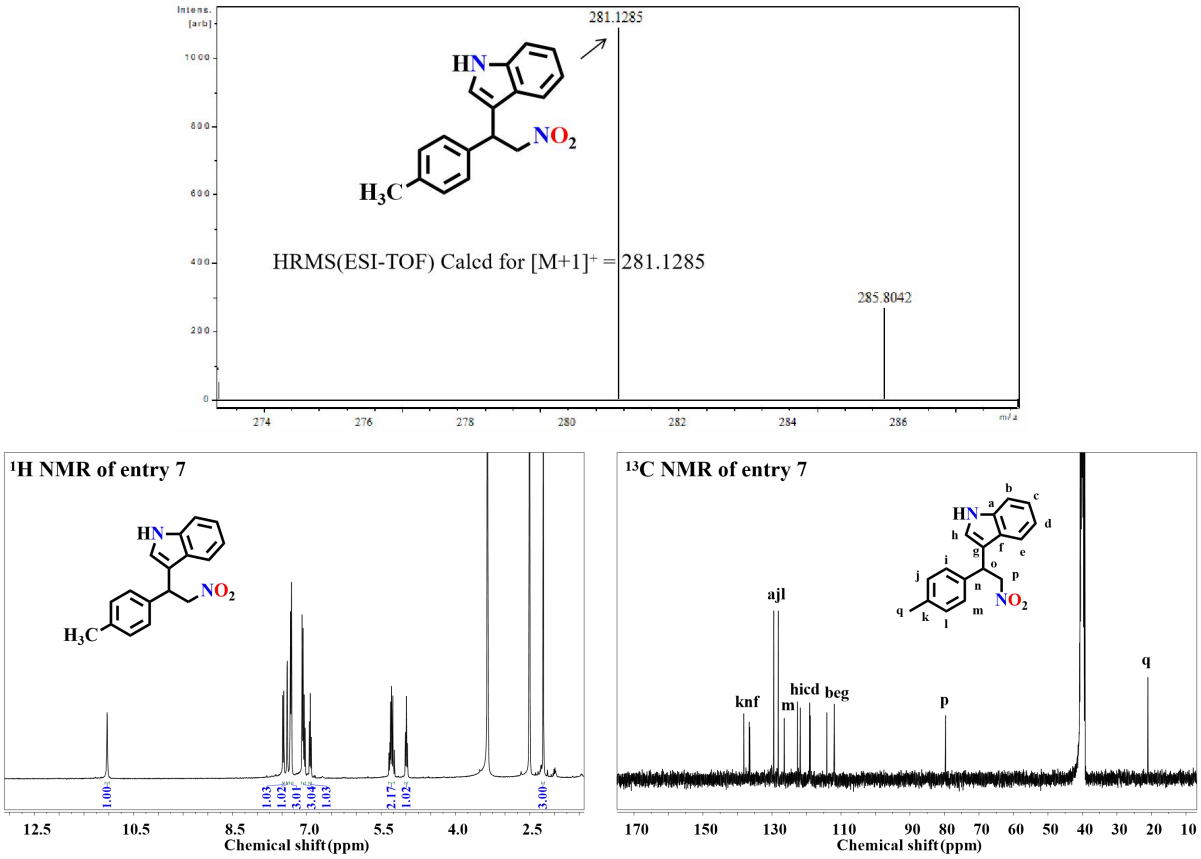

Fig. S14. HRMS, ^{1}H NMR and ^{13}C NMR spectra for 3-(2-nitro-1-(*p*-tolyl)ethyl)-1*H*-indole (Table 2, entry 7). HRMS (ESI): *m/z* $[M+H]^+$, Calcd for $C_{17}H_{16}N_2O_2^+$, 281.1286, found, 281.1285. ^{1}H NMR (400 MHz, DMSO-d_6): δ 11.03 (s, 1H), 7.48 (d, J = 7.9 Hz, 1H), 7.40 (d, J = 2.3 Hz, 1H), 7.32 (dd, J = 8.1, 2.9 Hz, 3H), 7.11-7.03 (m, 3H), 6.93 (s, 1H), 5.29 (dd, J = 10.3, 8.3 Hz, 2H), 4.99 (s, 1H), 2.23 (s, 3H). ^{13}C NMR (101 MHz, DMSO-d_6) δ = 138.16, 136.52, 129.46, 128.16, 126.43, 122.60, 121.78, 118.98, 114.09, 111.95, 79.68, 21.04.

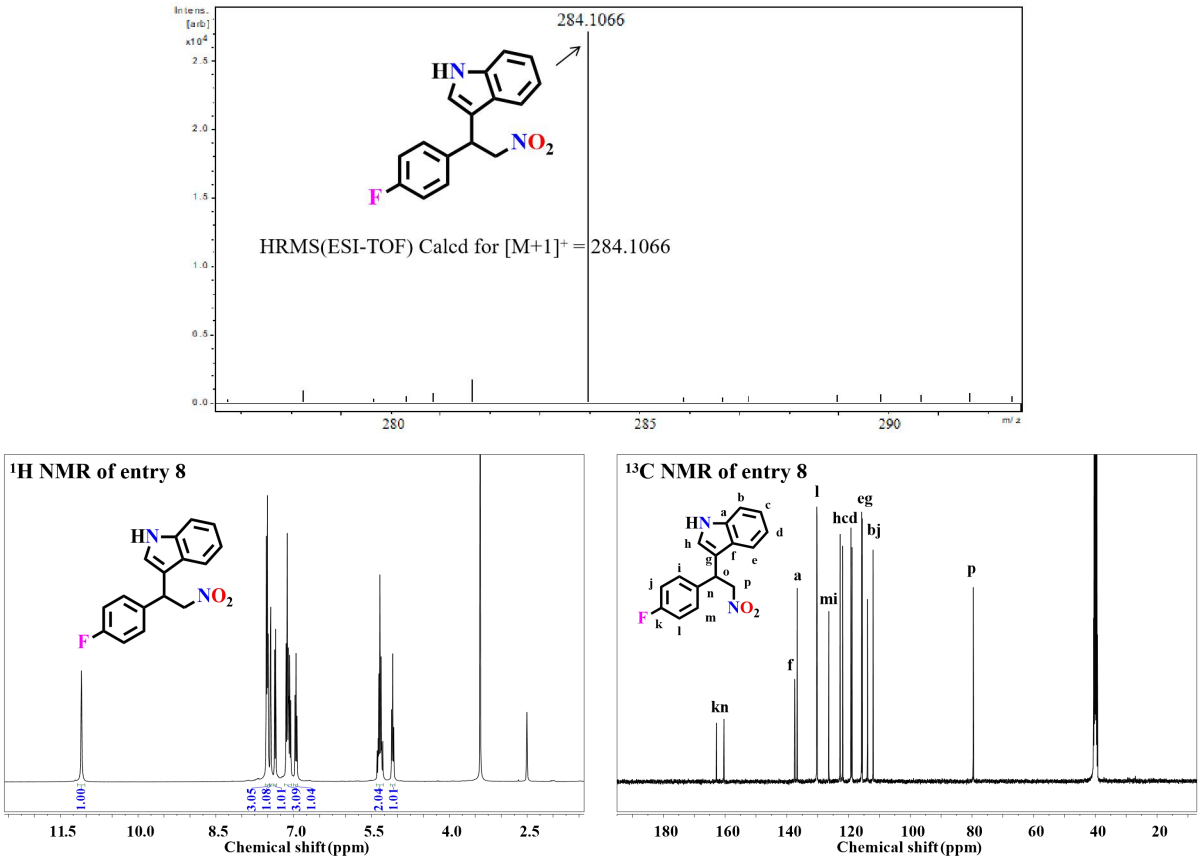

Fig. S15. HRMS, ^{1}H NMR and ^{13}C NMR spectra for 3-(1-(4-fluorophenyl)-2-nitroethyl)-1*H*-indole (Table 2, entry 8). HRMS (ESI): *m/z* $[M+H]^+$, Calcd for $C_{16}H_{14}N_2O_2^+$, 284.1086, found, 284.1066. ^{1}H NMR (400 MHz, DMSO-d_6): δ 11.09 (s, 1H), 7.55-7.46 (m, 3H), 7.45 (d, J = 2.2 Hz, 1H), 7.36 (d, J = 8.1 Hz, 1H), 7.10 (dt, J = 15.1, 8.2 Hz, 3H), 6.96 (t, J = 7.5 Hz, 1H), 5.41-5.27 (m, 2H), 5.09 (t, J = 8.2 Hz, 1H). ^{13}C NMR (101 MHz, DMSO-d_6) δ = 162.77, 160.35, 137.41, 136.64, 130.24, 126.37, 122.71, 121.89, 119.19, 118.85, 115.75, 115.54, 113.85, 112.02, 79.56.

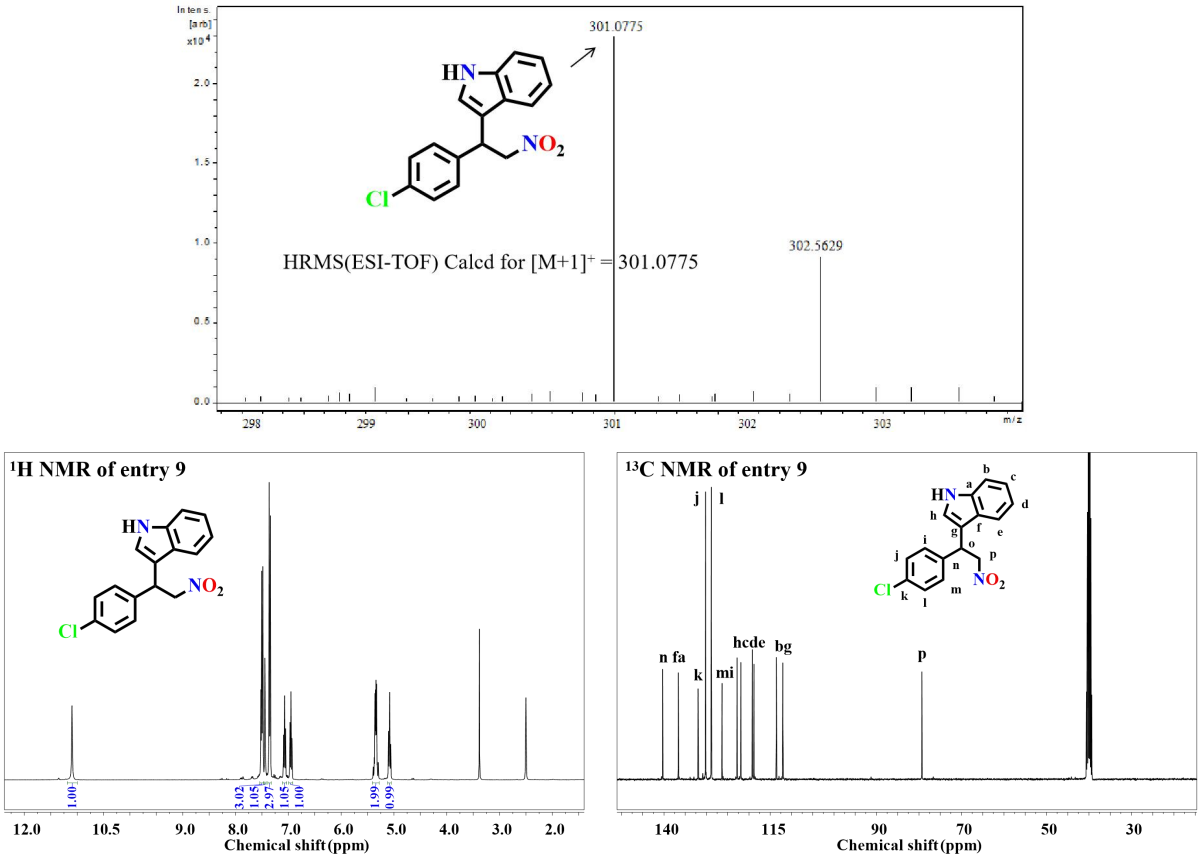

Fig. S16. HRMS, ^{1}H NMR and ^{13}C NMR spectra for 3-(1-(4-chlorophenyl)-2-nitroethyl)-1*H*-indole (Table 2, entry 9). HRMS (ESI): *m/z* $[M+H]^+$, Calcd for $C_{16}H_{13}ClN_2O_2^+$, 301.0786, found, 301.0775. ^{1}H NMR (400 MHz, DMSO-d_6): δ 11.10 (s, 1H), 7.54-7.47 (m, 3H), 7.44 (d, J = 2.3 Hz, 1H), 7.35 (d, J = 8.4 Hz, 3H), 7.07 (t, J = 7.3 Hz, 1H), 6.95 (t, J = 7.4 Hz, 1H), 5.41-5.28 (m, 2H), 5.08 (t, J = 8.2 Hz, 1H). ^{13}C NMR (101 MHz, DMSO-d_6) δ = 140.31, 136.63, 131.99, 130.22, 128.88, 126.33, 122.80, 121.91, 119.22, 118.83, 113.55, 112.04, 79.31.

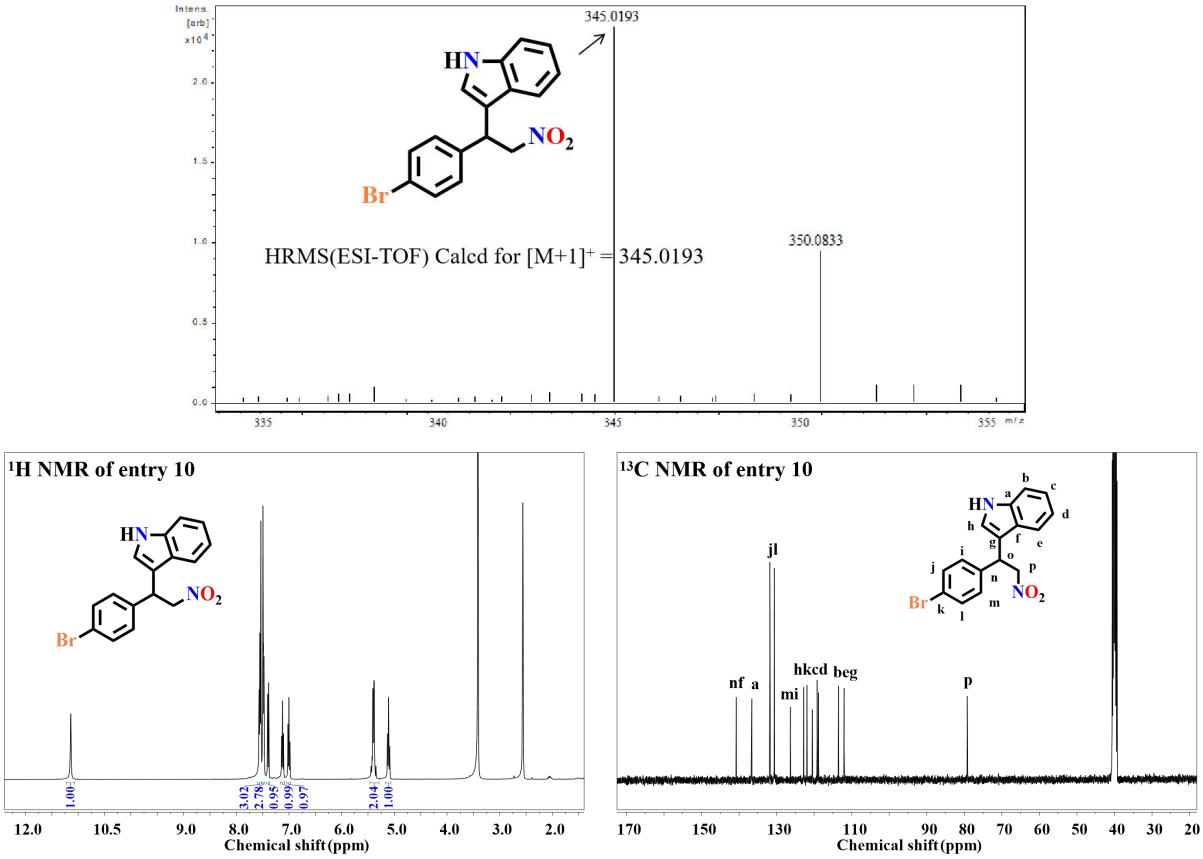

Fig. S17. HRMS, ^{1}H NMR and ^{13}C NMR spectra for 3-(1-(4-bromophenyl)-2-nitroethyl)-1*H*-indole (Table 2, entry 10). HRMS (ESI): *m/z* $[M+H]^+$, Calcd for $C_{16}H_{13}BrN_2O_2^+$, 345.0185, found, 345.0193. ^{1}H NMR (400 MHz, DMSO-d_6): δ 11.14 (s, 1H), 7.55 (dd, J = 7.9, 5.9 Hz, 3H), 7.48 (dd, J = 5.6, 2.9 Hz, 3H), 7.39 (d, J = 8.1 Hz, 1H), 7.12 (t, J = 7.2 Hz, 1H), 7.00 (t, J = 7.2 Hz, 1H), 5.40 (dd, J = 8.2, 3.0 Hz, 2H), 5.12 (d, J = 8.2 Hz, 1H). ^{13}C NMR (101 MHz, DMSO-d_6) δ = 136.61, 131.79, 130.60, 122.79, 121.91, 119.21, 118.82, 113.48, 112.02, 79.21.

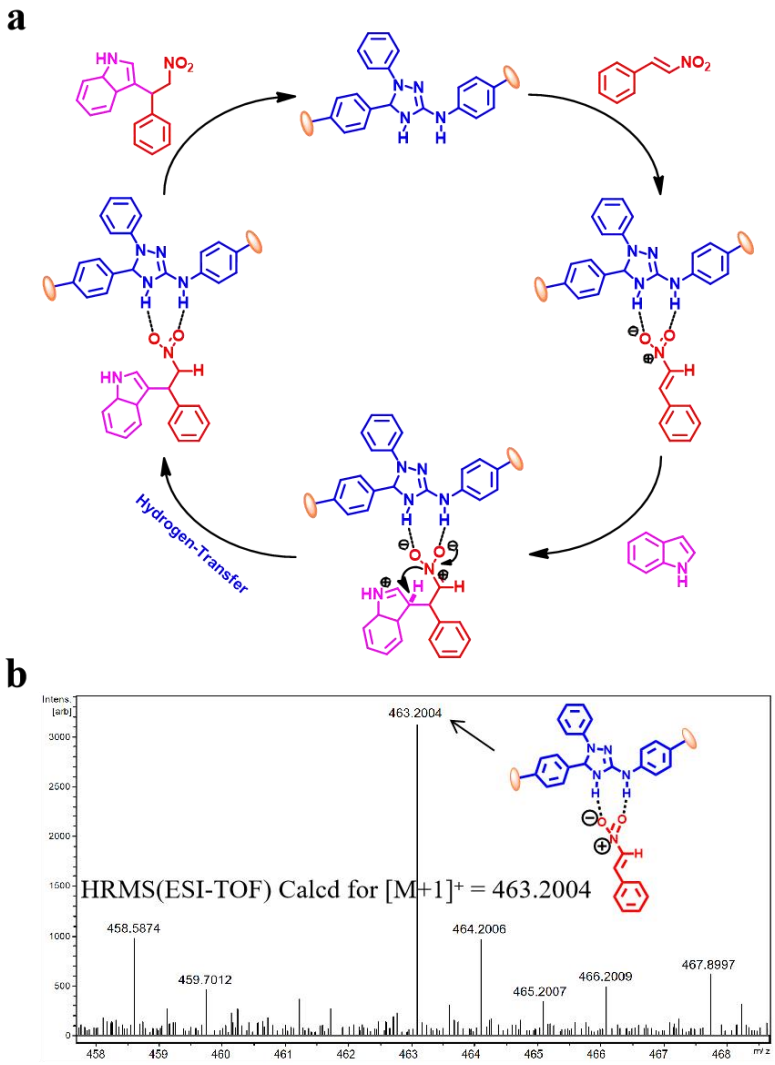

Fig. S18. The possible mechanism for the Friedel-Crafts alkylation of indole with *β*-nitrostyrene catalyzed by TBP-COF. **a)** The schematic diagram for possible mechanism. **b)** MS spectrum for the corresponding intermediate.

7. References

[1] S. Li, Y. Z. Liu, L. Li, C. X. Liu, J. N. Li, S. Ashraf, P. F. Li, B. Wang, *ACS Appl. Mater. Interfaces,* 2020, **12**, 22910−22916.

[2] C. F. Zhao, C. S. Diercks, C. H. Zhu, N. Hanikel, X. K. Pei, O. M. Yaghi, *J. Am. Chem. Soc.,* 2018, **140**, 16438−16441.

[3] M. Yusuf, S. Thakur, *J. Heterocyclic Chem.,* 2019, **56**, 3403−3413.

[4] A. Das, N. Anbu, M. SK, A. Dhakshinamoorthy, S. Biswas, *Inorg. Chem.,* 2019, **58**, 5163–5172.

[5] C. S. Schwalm, M. A. Ceschi, D. Russowsky, *J. Braz. Chem. Soc.,* 2011, **22**, 623–636.

[6] R. Mohammadian, M. M. Amini, A. Shaabani, *Catal. Commun.,* 2020, **136**, 105905.

[7] K. Moriyama, T. Sugiue, Y. Saito, S. Katsuta, H. Togo, *Adv. Synth. Catal.,* 2015, **357**, 2143–2149.

[8] G. Cera, D. Balestri, M. Bazzoni, L. Marchiò, A. Secchi, A. Arduini, *Org. Biomol. Chem.,* 2020, **18**, 6241–6246.

[9] L. Qi, *Russ. J. Org. Chem.,* 2020, **56**, 169–173.

[10] N. N. Wan, Y. H. Hui, Z. F. Xie, J. D. Wang, *Chin. J. Chem.,* 2012, **30**, 311–315.

[11] N. Nagarjun, P. Concepcion, A. Dhakshinamoorthy, *Appl. Organometal. Chem.,* 2020, **34**, e5578.

[12] X. P. Zhang, Z. J. Zhang, J. Boissonnault, S. M. Cohen, *Chem. Commun.,* 2016, **52**, 8585–8588.

[13] J. Ma, S. Ng, Y. Yong, X. Z. Luo, X. Wang, X. W. Liu, *Chem. Asian J.,* 2010, **5**, 778–782.

[14] X. Ji, H. Tong, Y. Yuan, *Synth. Commun.,* 2011, **41**, 372–379.

[15] C. W. Kuo, C. C. Wang, H. L. Fang, B. R. Raju, V. Kavala, P. M. Habib, C.-F. Yao, *Molecules*, 2009, **14**, 3952–3963.

[16] S. Sobhani, R. Jahanshahi, *New J. Chem.,* 2013, **37**, 1009–1015.

[17] L. Liang, Q. Liu, J. L. Zhang, F. Y. Wang, Y. Yuan, *Res. Chem. Intermed.,* 2013, **39**, 1957–1962.

[18] G. Bartoli, M. Bosco, S. Giuli, A. Giuliani, L. Lucarelli, E. Marcantoni, L. Sambri, E. Torregiani, *J. Org. Chem.,* 2005, **70**, 1941–1944.

[19] D. Markad, S. K. Mandal, *ACS Catal.,* 2019, **9**, 3165–3173.

[20] P. K. Singh, A. Bisai, V. K. Singh, *Tetrahedron lett.,* 2007, **48**, 1127–1129.

[21] A. Nagaraj, D. Amarajothi, *J. Colloid Interf. Sci.,* 2017, **494**, 282–289.

[22] G. K. Dam, S. Let, V. Jaiswal, S. K. Ghosh, *ACS Sustainable Chem. Eng.,* 2024, **12**, 3000−3011.

[23] M. Singh, S. Neogi, *Inorg. Chem. Front.,* 2024,**11**, 8866−8875.

[24] M. Jeganathan, K. Kanagaraj, A. Dhakshinamoorthy, K. Pitchumani, *Tetrahedron Lett.,* 2014, **55**, 2061−2064.

[25] M. Singh, S. Neogi, *Inorg. Chem.,* 2023, **62**, 871−884.